Low-energy electron scattering by N_2O

M. H. F. Bettega
Departamento de Física, Universidade Federal do Paraná, Caixa Postal 19044, 81531-990, Curitiba, Paraná, Brazil

C. Winstead and V. McKoy
A. A. Noyes Laboratory of Chemical Physics, California Institute of Technology, Pasadena, California 91125, USA
(Received 23 March 2006; published 8 August 2006)

We present elastic integral, differential, and momentum-transfer cross sections for electron collisions with N_2O. We show that, with a slight modification of a method of incorporating polarization effects proposed recently by us [Winstead, McKoy, and Bettega, Phys. Rev. A **72**, 042721 (2005)] along with a flexible one-particle basis set, we can reproduce features in the experimental data that were not reproduced by earlier calculations. We also find evidence of a Ramsauer-Townsend minimum, which our calculation places at about 0.2 eV.

DOI: 10.1103/PhysRevA.74.022711 PACS number(s): 34.80.Bm, 34.80.Gs

I. INTRODUCTION

Collisions of low-energy electrons with N_2O have been studied by numerous experimental and theoretical groups [1–14] in the past two decades. Earlier work [15–21] indicated the existence of two shape resonances in the low-energy cross section: one belonging to Π symmetry located around 2.4 eV, the other to Σ symmetry and located around 8 eV. Most of the recent calculations agree moderately well on these two features. There is also agreement between the calculated and measured elastic differential cross sections (DCSs) for energies of about 10 eV and above, even when polarization effects are omitted [10,11], while disagreement between the calculated and measured DCSs at or near the resonances can be attributed to the fixed-nuclei approximation. However, even for energies between ~3 and ~7 eV (i.e., between the two shape resonances), serious discrepancies are found between theory and experiment for scattering angles smaller than 60°. Kitajima and co-workers [12] emphasized that the minimum seen in the experimental DCSs at these energies had not been reproduced by any calculations. They also noted that similar features, which theory likewise failed to reproduce, were seen in many other molecules.

Three of the recent theoretical calculations incorporated polarization effects, namely, the *R*-matrix calculations of Sarpal and co-workers [7] and of Morgan and co-workers [9] and the calculations of Winstead and McKoy [10] using the Schwinger multichannel (SMC) method. Only the last two reported DCSs. Although these calculations used different treatments of polarization, they give fairly consistent results for the integral cross section below 10 eV, with the exception that the calculations of Morgan and co-workers show no Σ resonance there. It is therefore both surprising and a challenge to theory that they do not, as mentioned above, reproduce the measured DCSs at nonresonant energies, especially since *all* of the experimental DCSs [4–6,12] agree with each other; in particular, Kitajima and co-workers [12] report DCSs obtained from two independent measurements on different apparatuses that agree very well.

Our main purpose in the present paper is to explore what further steps are needed to bring calculated DCSs between ~3 and ~7 eV into agreement with experiment for N_2O, especially at scattering angles below 60°. In so doing, we also hope to provide good-quality calculated cross sections for low-energy electron scattering by N_2O. This work is a continuation of our earlier work on e^--C_2H_4 collisions [23], where we addressed a similar feature in the cross section [22], and it employs similar techniques, with some slight variations that will be described below.

The next section discusses our computational procedure, with emphasis on the treatment of polarization effects and the construction of the one-electron basis set. This is followed by a presentation and discussion of our results and a brief conclusion.

II. COMPUTATIONAL PROCEDURES

Our scattering calculations were performed with the Schwinger multichannel method [24] implemented for parallel computers [25,26]. General features of the SMC method can be found in the references cited. Here we are interested in the representation of polarization and other details specific to the present calculations.

In the SMC method, the direct configuration space, describing a free electron and the unperturbed molecular charge density, is constructed as follows:

$$\{\chi_i\} = \{\mathcal{A}(\Phi_1 \otimes \varphi_i)\} \tag{1}$$

where Φ_1 is the *N*-electron Hartree-Fock wave function for the target ground state, φ_i is a one-electron function unoccupied in Φ_1 (a virtual orbital), and $\mathcal{A}$ is the antisymmetrizer. Polarization effects are taken into account by enlarging the configuration space to include configuration-state functions (CSFs) of the type

$$\{\chi_{ju}\} = \{\mathcal{A}(\Phi_j \otimes \varphi_u)\}, \quad j \geq 2, \tag{2}$$

where Φ_j are *N*-electron configurations that are singly excited (from a "hole" orbital into a "particle" orbital) relative to Φ_1, and the φ_u are again one-electron functions chosen from the virtual-orbital space. The efficient choice of hole, particle, and scattering orbitals is a critical issue in practice and will be discussed next.

In our recent study of electron collisions with C_2H_4 [23], we noted the advantages of modified virtual orbitals (MVOs) as particle orbitals. MVOs are generated by the diagonalization, in the virtual-orbital space, of a closed-shell cation Fock operator formed by removing electrons from Φ_1 [30]. They therefore retain the desirable orthogonality properties of the Hartree-Fock virtual orbitals but are ordered in such a way that the lowest-energy MVOs are compact and valencelike. This ordering provides a natural scheme for systematically improving the representation of polarization. In seven of the eight irreducible representations of C_2H_4, we used the lowest 30 MVOs as particle orbitals and all six valence occupied orbitals as hole orbitals to form singlet-coupled states Φ_j. In the strongly shape-resonant B_{2g} symmetry, we used only the first MVO as a particle orbital to form all singlet- or triplet-coupled excitations from the valence orbitals. Our purpose was to avoid overcorrelation of the B_{2g} resonance that might place it too low in energy.

In the present study of N_2O, we found it necessary to modify slightly the procedure described above. Instead of using different approaches to resonant and nonresonant symmetries, we use the *same* approach for *each* symmetry: namely, that used for the nonresonant or weakly resonant symmetries of C_2H_4. We believe that the key difference between the two molecules is the lower effective symmetry of N_2O. Because we work with Cartesian Gaussian orbitals and N_2O lacks an inversion center, its effective symmetry is C_{2v}, in contrast to the D_{2h} symmetry of C_2H_4. In particular, the B_1 and B_2 representations contain, for N_2O, contributions that would separate, in a more symmetric molecule such as CO_2, into resonant Π_g and nonresonant Π_u components. Trial of different configuration-selection schemes indicated that including a sufficient representation of nonresonant polarization in B_1 and B_2 was a more important consideration than was avoiding overcorrelation of the $^2\Pi$ resonance.

The calculations were performed with the nuclei fixed at their ground-state equilibrium geometry, as in previous work [10]. To construct the target ground state and the set of MVOs, we used the package GAMESS [27] and its TZV+G(3*d*) basis set with default exponents and splitting factors for the diffuse and polarization functions [27,31]. We worked in the C_{2v} subgroup of the full $C_{\infty v}$ group. The MVOs were generated by diagonalizing a +4 cationic Fock operator. In each representation of C_{2v}, our hole-particle space included all singlet excitations from the eight valence occupied orbitals into the lowest 30 MVOs.

In C_2H_4, we found that adding basis functions on a grid of extra centers noticeably improved the description of forward scattering but was not critical to obtaining the minimum in the small-angle DCS. Such extra centers are more important in N_2O, possibly because the basis functions located on the H atoms in C_2H_4 already bring in some longer-range and higher partial-wave contributions that are absent in an ordinary N_2O basis set. In particular, since N_2O is linear and the TZV+G(3*d*) basis set contains only *s*-, *p*-, and *d*-type functions, it includes only partial waves with azimuthal quantum numbers up to $m=2$. We tested the importance of higher azimuthal quantum numbers by performing three calculations differing in their use of additional Cartesian Gaussian functions placed on extra (chargeless) centers with locations chosen to produce $m=3$ partial-wave contributions while retaining C_{2v} symmetry. The first calculation used no extra centers, while in the second, 24 extra centers were added at the vertices of four hexagons with sides equal to 1.1 Å that were placed in planes perpendicular to the internuclear axis and halfway between or half a bond length beyond the nuclei. In the third calculation, we further included 18 centers located at the vertices of three larger hexagons (sides equal to 2.2 Å) centered on the nuclei, plus two extra centers located on the molecular axis but beyond the N and O atoms by distances equal to the N-N and N-O bond lengths, respectively. At each extra center, we placed one *s*-type Gaussian function with exponent 0.144 and one *p*-type function with exponent 0.2. Table I shows the number of Cartesian Gaussian functions and the number of CSFs employed in each calculation.

TABLE I. Numbers of Cartesian Gaussian functions (NCGFs) and configuration-state functions (NCSFs) used in the scattering calculations (see text for discussion).

	No extra centers		24 extra centers		44 extra centers	
Symmetry	NCGF	NCSF	NCGF	NCSF	NCGF	NCSF
A_1	108	12162	204	11602	284	14995
B_1	108	9199	204	10821	284	14468
B_2	108	9199	204	10685	284	13798
A_2	108	4985	204	9925	284	13292

N_2O has a small permanent dipole moment of 0.161 D [28]. Our calculated value, obtained with the larger basis set described above, is 0.618 D. We did not include an explicit correction for long-range, dipolar scattering. Because the calculated dipole is larger than the experimental value, including the dipole interaction through the usual closure procedure [29] would probably make the results worse rather than better, and, at any rate, the correction would be significant only at very low energies or extreme forward angles. In addition, the extra centers should bring in dipole scattering up to a fairly high angular momentum (i.e., a fairly large impact parameter). We note that, although the partial-wave expansion of the elastic scattering amplitude for a fixed dipole is formally divergent at all angles, no special measures are needed to obtain finite results, both because we compute the amplitude in the plane-wave representation and because we use a square-integrable representation of the wave function, which effectively discards the (unphysical) contribution from scattering at arbitrarily large impact parameters that leads to divergence when rotation is neglected.

III. RESULTS AND DISCUSSION

In Fig. 1 we compare our calculated DCSs at 4, 5, 6, 7, 8, and 10 eV obtained in the three different calculations described above. The inclusion of extra centers that can represent partial waves up to $m=3$ is clearly crucial for describing the minimum in the DCSs below 60°. However, Fig. 1 also shows that increasing the number of centers from 24 to 44

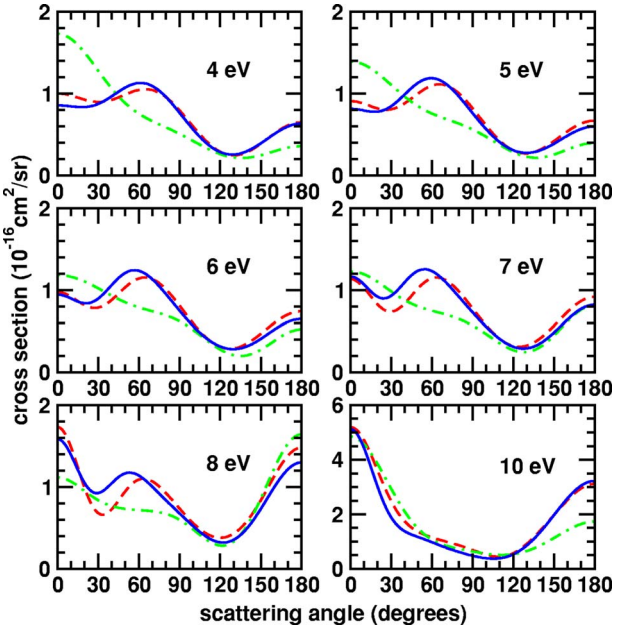

FIG. 1. (Color online) Differential cross sections for N_2O at 4, 5, 6, 7, 8, and 10 eV. Dot-dashed line (green), our results with no extra centers; dashed line (red), our results with 24 extra centers; solid line (blue), our results with 44 extra centers.

did not make a significant difference in the results. Although not shown, the integral and momentum-transfer cross sections obtained in these different calculations were in close agreement. From here on, we will show only what we consider our best results, namely, those obtained with 44 extra centers.

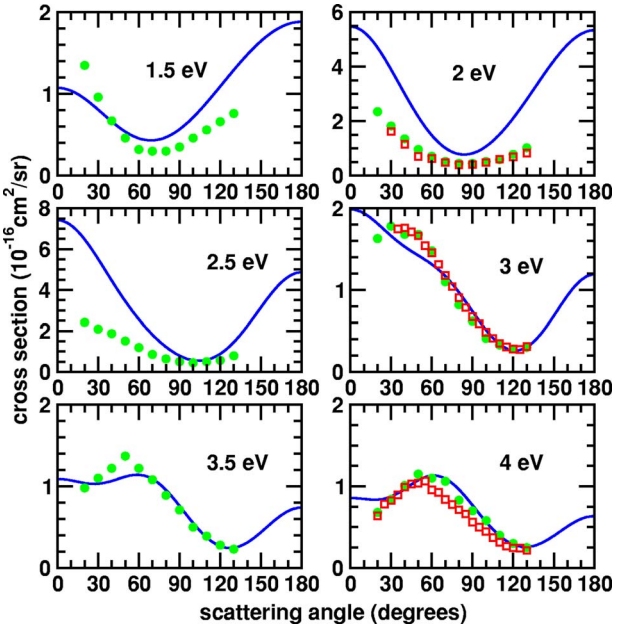

FIG. 2. (Color online) Differential cross sections for N_2O at 1.5, 2, 2.5, 3, 3.5, and 4 eV. Solid line (blue), our results with 44 extra centers; circles (green) experimental data from Ref. [12] obtained at Sophia University; squares (red), experimental data from Ref. [12] obtained at the Australian National University.

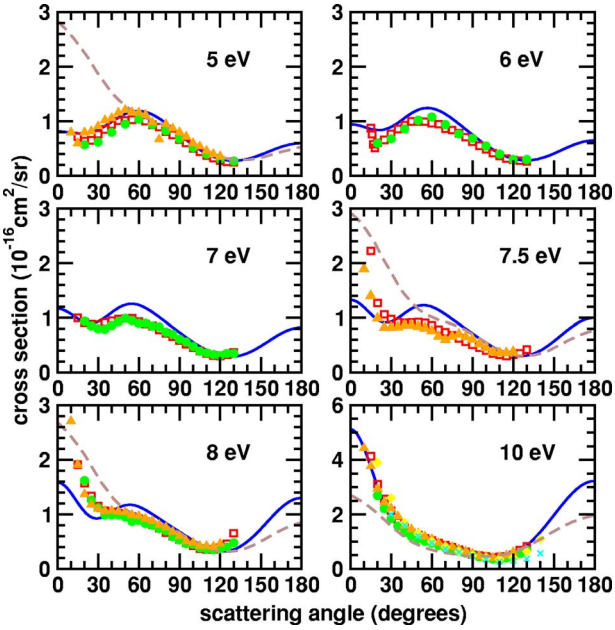

FIG. 3. (Color online) As in Fig. 2 at 5, 6, 7, 7.5, 8, and 10 eV and with the following additional results: diamonds (yellow), experimental data from Ref. [4]; triangles (orange), experimental data from Ref. [5]; crosses (light blue), experimental data from Ref. [6]; dashed line (brown), calculations from Ref. [9].

Figures 2–4 compare our calculated DCSs for energies from 1.5 to 15 eV with experimental data [4–6,12] and with the results of *R*-matrix calculations [9]. Figure 2 compares our results with the measurements of Kitajima and coworkers [12] for energies from 1.5 to 4 eV. At 1.5 eV, there is some agreement between theory and experiment, but at 2 and 2.5 eV, around the $^2\Pi$ shape resonance, the agreement worsens because of our neglect of nuclear motion. The

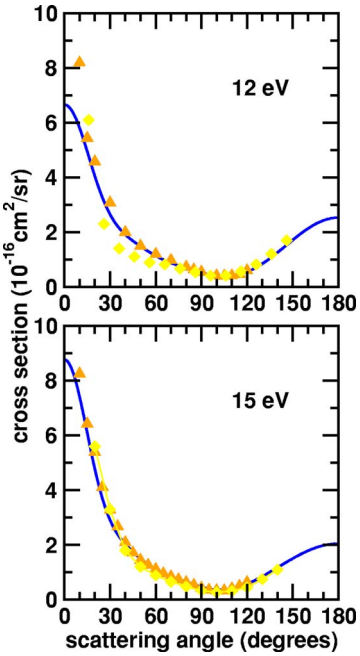

FIG. 4. (Color online) As in Fig. 3 at 12 and 15 eV.

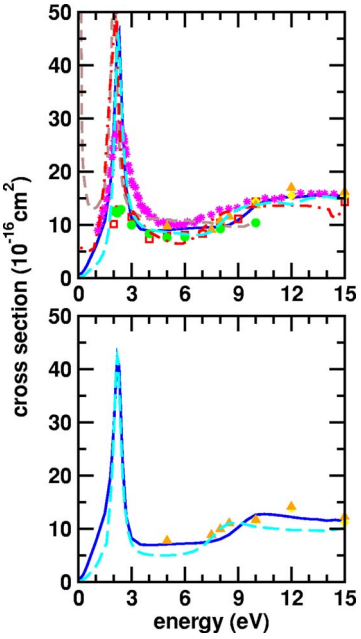

FIG. 5. (Color online) Integral (upper panel) and momentum-transfer (lower panel) cross sections for N_2O. Solid line (blue), our results with 44 extra centers; stars (pink), experimental total cross section from Ref. [3]; diamonds (yellow), experimental data from Ref. [4]; triangles (orange), experimental data from Ref. [5]; circles (green) experimental data from Ref. [12] obtained at Sophia University; squares (red), experimental data from Ref. [12] obtained at the Australian National University; dot-dashed line (red), theoretical results from Ref. [7]; short-dashed line (brown), theoretical results from Ref. [9]; long-dashed line (light blue), theoretical results from Ref. [10].

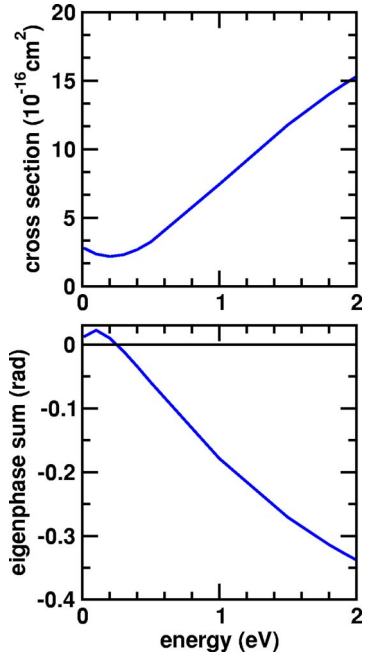

FIG. 6. (Color online) Integral cross section for the A_1 symmetry (upper panel) and the corresponding eigenphase sum (lower panel).

small-angle minimum appears in the measured DCS at 3 eV but not in our calculated DCS, though we do see fairly good agreement for angles above 60°. On the other hand, at still higher energies, the calculations do begin to exhibit a minimum, and at 3.5 and 4 eV, the agreement with the experiment in the small-angle region improves. In Fig. 3, we compare our results from 5 to 10 eV with various measurements [4–6,12] and with the calculations of Morgan and co-workers [9]. At 5, 6, and 7 eV, the agreement between our results and experiment is very good at all angles, though at 6 and 7 eV the calculated DCS appears to be too large around the maximum at ~60°. At 7.5 and 8 eV we are again in the vicinity of a shape resonance (the Σ resonance), and the agreement between our results and the measurements deteriorates, but at 10 eV it is again very good. One can see from Fig. 3 that the *R*-matrix results of Morgan and co-workers [9] do not describe the minimum in the DCSs, nor did our own earlier calculations [10] (not shown). In fact, comparing Figs. 1 and 3, we see qualitative similarity between the DCSs of Morgan and co-workers and our results obtained without extra centers (although the latter are much smaller in the forward direction and thus in better quantitative agreement with the measured DCSs).

Figure 4 shows the DCSs at 12 and 15 eV. At these energies, the agreement between our results and the experimental data [4,5] is good, except at small scattering angles, where our results lie below the experiment, possibly due to basis-set limitations and/or to our neglect of corrections for long-range scattering from the (small) dipole moment of N_2O.

Integral and momentum-transfer cross sections are shown in Fig. 5. Despite including a much more extensive set of configurations in B_1 and B_2 symmetries to represent polarization effects, our present calculations place the $^2\Pi$ shape resonance at nearly the same energy as did our previous study [10], close to the peak in the total cross section measured by Szmytkowski and co-workers [3]. The two *R*-matrix calculations [7,9] place the shape resonance energy slightly lower but still close to the observed peak. As seen in Fig. 5, the calculated integral elastic and momentum-transfer cross sections reproduce the shape and magnitude of the experimental data fairly well above the $^2\Pi$ resonance energy.

In Fig. 6 we show the A_1 contribution to the integral cross section from 0 to 2 eV, along with the corresponding eigenphase sum. At these energies, by far the dominant contribution to A_1 comes from Σ symmetry. A minimum is clearly visible in the cross section near 0.2 eV, where the eigenphase sum changes sign, behavior characteristic of a Ramsauer-Townsend (RT) minimum. A low-energy minimum has indeed been observed in the total electron cross section [16,19] and, more recently, in the elastic differential cross section at 135° [14]. However, one expects a rise in the e^--N_2O cross section at very low energy due to scattering by the dipole potential, so the experimental results can be, and have been, explained without invoking the RT mechanism. We also note that inclusion of corrections for dipolar scattering would alter our low-energy cross section. Thus the present results at most suggest, rather than demonstrate, the presence of a RT minimum in N_2O.

IV. CONCLUDING REMARKS

The results in Figs. 1–3 demonstrate that we are able to reproduce the minima in the experimental DCSs of N_2O using excitations from valence orbitals into the lowest MVOs to represent polarization, as was the case for C_2H_4 [23]. The present results thus give further evidence for the utility of MVOs as a simple, effective, systematically extensible particle basis. For both C_2H_4 and N_2O, use of a distributed one-electron basis set improves the results; in N_2O, however, we found that the distributed basis was essential to obtaining qualitatively correct DCSs, which was not the case in C_2H_4. We believe the difference may be that in C_2H_4 we already have off-axis functions (centered on the H atoms) before adding the extended basis, whereas in N_2O we start with only on-axis functions having $m \leq 2$. A second difference arises in the treatment of polarization in the symmetries containing the π^* resonance. For C_2H_4, including only relaxation of the target in the presence of an electron trapped in the resonance orbital worked well. For N_2O, that approach gives a good location for the $^2\Pi$ resonance but an inadequate description of higher-energy scattering. Here the difference is probably the lack of an inversion center in N_2O. In C_2H_4, the π^* resonance belongs to a representation whose leading partial wave is d ($\ell=2$) and which contributes only a weak background away from resonance. In N_2O, the leading wave in the representation containing the π^* resonance is p ($\ell=1$), and it is natural that both background scattering and the influence of polarization on that background should be stronger. Indeed, we saw in C_2H_4 that polarization effects on the $\ell=1$ wave were very strong [23].

The present calculations, taken together with our C_2H_4 results, indicate that the previous failure of calculations to reproduce the low-angle minimum seen in elastic electron scattering by various molecules [12] arises from an insufficient representation of polarization effects, sometimes in combination with an inadequate one-electron basis set. Possible explanations that have been considered in the past, including target correlation effects, vibrational effects, and explicit coupling to open electronic-excitation channels, would have entailed calculations of considerably increased complexity and difficulty. Fortunately, shortcomings in the polarization space and one-electron basis set are more readily corrected using current methodology, as we have shown.

ACKNOWLEDGMENTS

M.H.F.B. acknowledges support from the Brazilian agency Conselho Nacional de Desenvolvimento Científico e Tecnológico (CNPq) under NSF/CNPq Project No. 490166/2003-2 and from the Paraná State Agengy Fundação Araucária. C.W. and V.M. acknowledge support from U.S. Department of Energy, Office of Basic Energy Sciences, and U.S. National Science Foundation, Office of International Science and Engineering. M.H.F.B. acknowledges computational support from FINEP under Project No. CT-Infra 1 and also from Professor Carlos de Carvalho at DFis-UFPR. The authors acknowledge computational support from the Caltech-JPL Supercomputing Project and the Caltech Center for Advanced Computing Research (CACR). M.H.F.B. thanks Professor Marco A. P. Lima for helpful conversations.

[1] L. Andrić and R. I. Hall, J. Phys. B **17**, 2713 (1984).
[2] Ch. K. Kwan, Y.-F. Hsieh, W. E. Kauppila, S. J. Smith, T. S. Stein, M. N. Uddin, and M. S. Dababneh, Phys. Rev. Lett. **52**, 1417 (1984).
[3] Cz. Szmytkowski, G. Karwasz, and K. Maciąg, Chem. Phys. Lett. **107**, 481 (1984).
[4] B. Marinković, Cz. Szmytkowski, V. Pejčev, D. Filipović, and L. Vušković, J. Phys. B **19**, 2365 (1986).
[5] W. M. Johnstone and W. R. Newell, J. Phys. B **26**, 129 (1993).
[6] M. Kubo, D. Matsunaga, T. Suzuki, and H. Tanaka, in *Abstracts of Contributed Papers of the 12th International Conference on the Physics of Electronic and Atomic Collisions, Gatlinburg, 1981*, edited by S. Datz (North-Holland, Amsterdam, 1981), p. 360.
[7] B. K. Sarpal, K. Pfingst, B. M. Nestmann, and S. D. Peyerimhoff, J. Phys. B **29**, 857 (1996).
[8] S. E. Michelin, T. Kroin, and M.-T. Lee, J. Phys. B **29**, 2115 (1996).
[9] L. A. Morgan, C. J. Gillan, J. Tennyson, and X. Chen, J. Phys. B **30**, 4087 (1997).
[10] C. Winstead and V. McKoy, Phys. Rev. A **57**, 3589 (1998).
[11] S. M. S. da Costa and M. H. F. Bettega, Eur. Phys. J. D **3**, 67 (1998).
[12] M. Kitajima, Y. Sakamoto, R. J. Gulley, M. Hoshino, J. C. Gibson, H. Tanaka, and S. J. Buckman, J. Phys. B **33**, 1687 (2000).
[13] M.-T. Lee, I. Iga, M. G. P. Homem, L. E. Machado, and L. M. Brescansin, Phys. Rev. A **65**, 062702 (2002).
[14] M. Allan and T. Skalický, J. Phys. B **36**, 3397 (2003).
[15] E. Brüche, Ann. Phys. **83**, 1065 (1927).
[16] C. Ramsauer and R. Kollath, Ann. Phys. **7**, 176 (1930).
[17] G. J. Schulz, J. Chem. Phys. **34**, 1778 (1961).
[18] P. J. Chantry, J. Chem. Phys. **51**, 3369 (1969).
[19] A. Zecca, I. Lazzizzera, M. Krauss, and C. E. Kuyatt, J. Chem. Phys. **61**, 4560 (1974).
[20] R. Azria, S. F. Wong, and G. J. Schulz, Phys. Rev. A **11**, 1309 (1975).
[21] M. Tronc, L. Malegat, R. Azria, and Y. Lecoat, in *Abstracts of Contributed Papers of the 12th International Conference on the Physics of Electronic and Atomic Collisions, Gatlinburg, 1981* (Ref. [6]), p. 372.
[22] R. Panajotovic, M. Kitajima, H. Tanaka, M. Jelisavcic, J. Lower, L. Campbell, M. J. Brunger, and S. J. Buckman, J. Phys. B **36**, 1615 (2003).
[23] C. Winstead, V. McKoy, and M. H. F. Bettega, Phys. Rev. A **72**, 042721 (2005).
[24] K. Takatsuka and V. McKoy, Phys. Rev. A **24**, 2473 (1981); **30**, 1734 (1984).
[25] C. Winstead and V. McKoy, Adv. At., Mol., Opt. Phys. **36**, 183 (1996).

[26] C. Winstead and V. McKoy, Comput. Phys. Commun. **128**, 386 (2000).
[27] M. W. Schmidt, K. K. Baldridge, J. A. Boatz, S. T. Elbert, M. S. Gordon, J. H. Jensen, S. Koseki, N. Matsunaga, K. A. Nguyen, S. J. Su, T. L. Windus, M. Dupuis, and J. A. Montgomery, J. Comput. Chem. **14**, 1347 (1993).
[28] *CRC Handbook of Chemistry and Physics*, 79th ed., edited by D. R. Lide (CRC, Boca Raton, FL, 1998).
[29] T. N. Rescigno and B. I. Schneider, Phys. Rev. A **45**, 2894 (1992), and references therein.
[30] C. W. Bauschlicher, J. Chem. Phys. **72**, 880 (1980).
[31] T. H. Dunning, J. Chem. Phys. **55**, 716 (1971).